


 Cite this: *Sens. Diagn.*, 2025, 4, 966

 Received 25th June 2025,  
 Accepted 30th August 2025

DOI: 10.1039/d5sd00110b

[rsc.li/sensors](https://rsc.li/sensors)

## Towards electrochemical sensing of gemcitabine release from hybrid nanoparticles in pancreatic cancer cells

 Adeolu Oluwasanmi, Kelly Brown,  Clare Hoskins \* and Lynn Denny \*

**Theranostic clinical translation has been hindered by the lack of analytical tools facilitating interrogation. Here we report the detection of a chemotherapeutic agent, gemcitabine, released via heat trigger, from a hybrid iron oxide–gold theranostic nanoparticle surface *in vitro* in pancreatic cancer cells by electrochemiluminescence directly addressing this analytical gap.**

Pancreatic cancer has been classified as a cancer of unmet need. One substantial problem is the large lag time between diagnosis and treatment, therefore a single use platform which can both diagnose and treat could greatly enhance patient survival rate. Advancements in the knowledge and fabrication of nanotechnologies have led to one particularly exciting and innovative development for use in cancer diagnostics and therapeutics. These multifunctional nanoparticles are termed ‘theranostics’ which offer simultaneous diagnosis and therapeutic delivery.<sup>1,2</sup> This is particularly important not only for patient treatment time after diagnosis, but also as a mechanism to reduce the economic burden felt by the health services worldwide by reducing administrative costs between departments and patient bed time. A host of formulations based on hybrid nanoparticles (HNPs) have been developed with a focus on pancreatic cancer.<sup>3–5</sup> HNPs consist of a magnetic iron oxide, Fe<sub>3</sub>O<sub>4</sub>, core surrounded by a complete gold shell. These particles have shown potential for use as thermally activated drug delivery systems.<sup>1,2</sup> The multicomponent nature of these nanoparticles renders them not only suitable as imaging agents *via* magnetic resonance imaging (MRI) but also the ability to act as heat sources after laser irradiation of the gold surface. The intention is that after the HNPs have accumulated within the tumour tissue and cancer is confirmed by the clinician, that the particles can be activated rapidly using laser light, resulting in drug release

directly at the site of need. This reduces the off-target effects of these very potent chemotherapies and results in a rapid, more effective system. HNPs particles have shown potential for use as thermally activated drug delivery systems in this manner by coupling chemotherapies onto their surface either by electrostatic coupling or *via* more sophisticated thermally labile conjugation.<sup>3–5</sup> Studies have reported in depth on the fabrication, optimization, characterisation and physical properties of these systems previously.<sup>6,7</sup> The HNPs have been tested for their biocompatibility and heating effect both in phantom cells<sup>8</sup> and cadavers.<sup>9</sup> The effect of laser irradiation at 1064 nm and at various HNP concentrations on the cellular state of pancreatic adenocarcinoma cells and any resultant heat shock protein production has been determined.<sup>9</sup> These systems can be used as drug carriers (~120 nm) and release their payload upon laser irradiation with enhanced *in vivo* efficacy compared with free drug.<sup>4,5</sup> Gemcitabine (GEM) used to be the first line drug treatment for pancreatic cancer, but now is often given in combination therapy. By trafficking the drug into the cells on the HNP surface, it allows for increased efficiency of delivery and enhanced efficacy. Oluwasanmi *et al.* reported the introduction of a reversibly conjugated linker between the HNPs and GEM,<sup>4</sup> whereby, heat generation resulting from laser irradiation of the HNPs promoted linker breakdown *via* a retro Diels Alder reaction, resulting in prodrug (GEM modified with a maleimide linker, L-GEM) liberation. *In vitro* evaluation in pancreatic adenocarcinoma cells, showed the L-GEM was 4.3 times less cytotoxic than GEM, but exhibited 11-fold improvement in cellular uptake. *In vivo* the heat released L-GEM formulation outperformed free GEM with a 56% reduction in tumour size in pancreatic xenografts, as illustrated in Fig. 1.<sup>4</sup> Whilst this thermally triggered system shows great promise as a potential future theranostic, little is known of the drug fate after laser induced release, and currently there is no viable way to monitor this in real-time. This essential knowledge gap requires attention before clinical translation can occur. One such technique which may offer assistance in this area is electrochemiluminescence (ECL).

Department of Pure and Applied Chemistry, University of Strathclyde, Technology Innovation Centre, 99 George Street, Glasgow, G1 1RD, UK.  
 E-mail: [clare.hoskins@strath.ac.uk](mailto:clare.hoskins@strath.ac.uk), [lynn.denny@strath.ac.uk](mailto:lynn.denny@strath.ac.uk)





**Fig. 1** Iron oxide-gold hybrid theranostic nanoparticles (HNPs) decorated with a gemcitabine prodrug (L-GEM), attached via a maleimide-furan Diels Alder cycloadduct which is reversible upon elevated temperatures. A) Schematic representation, B) L-GEM release from HNP at elevated temperature in solution, C) effect of tumour size and D) tumour volume after 1 dose per week for 4 weeks on a pancreatic xenograft tumour exposed to HNP, L-GEM and HNP-L-GEM with and without pulsed laser irradiation at 1064 nm. Reprinted (adapted) with permission from ref. 1. Copyright 2017 Elsevier.

ECL is a diagnostic technique which uses the power of both electrochemical reactions and luminescence, combining these to produce light.<sup>10</sup> ECL has previously been reported also in cell visualization, in the study of proteins and other biomolecules as well as in the detection on drug molecules.<sup>10–14</sup> Prior works have successfully demonstrated the capability of ECL as a detection and monitoring strategy for GEM.<sup>15,16</sup> Osmium based luminophores facilitated the direct detection of GEM down to therapeutic levels (26  $\mu\text{M}$ ) within human pooled serum,<sup>17</sup> while inclusion of gold nanoparticles (AuNPs) demonstrated an electro-catalytic enhancement increasing the detection limit 60-fold with the traditional ruthenium luminophore.<sup>16</sup> Both these studies have proven the feasibility of ECL as a suitable detection mechanism for the monitoring of GEM within a patients' circulatory system and provide confidence toward *in vitro* analysis. Here, we exploit the power of ECL using the same fundamental strategies as previously reported to investigate the *in vitro* analysis of GEM as an imaging strategy to indicate the therapeutic drug release off an HNP surface upon heat generation. ECL controlled luminescence properties lend themselves well for such a methodology given the spatial and potential control offered without the need for an external light source.<sup>17,18</sup> Application of an external potential initiates the required chemical reactions, leading to the highly energetic electron transfer processes which are responsible for the production of light. This light can then be visually monitored and correlated to the presence of a target analyte. As such, ECL stands to offer a direct monitoring strategy for drug release, in this instance for GEM which behaves as the necessary co-reactant required for analysis.

In this study we trial the use of ECL to image the drug fate after heat initiated retro-Diels Alder triggered release of GEM

from the HNP surface. By utilising the EC behaviour of the drug, kinetic interactions between the nanoparticle and the drug, and the distance dependence of this reaction, we can image the location of drug after delivery. The kinetic requirements of this will allow for selective as well as sensitive imaging even in complex matrices. Initial work will require an electrode close to the nanoparticle but application of wireless bipolar EC will facilitate the understanding of drug fate after triggered release which is required before clinical translation of these exciting novel theranostic platforms.

## Materials and methods

Gemcitabine HCl, maleic anhydride was purchased from Fluorochem UK Ltd. All other chemicals were purchased from Alfa Aesar, UK unless otherwise stated and were at least ACS reagent grade or greater purity. HPLC grade organic solvents used for chemical synthesis and analysis, as well as cell culture media and supplements were purchased from Fisher Scientific, UK. BxPC-3 cells were purchased from LGC Standards, UK. Tris(2,2'-bipyridyl)-(dichlororuthenium(II)) hexahydrate ( $[\text{Ru}(\text{bpy})_3]^{2+}$ ), sodium chloride (NaCl) and 117 Nafion (~5% mixture of lower aliphatic alcohols) were purchased from Sigma Aldrich.

### Synthesis of HNP-GEM

GEM coated HNPs were synthesized and characterized as already reported previously.<sup>4</sup>

### Electrochemical analysis

All electrochemical and corresponding photoluminescence measurements were performed with a PalmSens 4 potentiostat coupled to a Hamamatsu H10723-20 photomultiplier tube



(PMT), housed within a light tight Faraday cage. Photoluminescence measurements were performed *via* a specially designed sensor holder which positions the PMT window directly above the working electrode surface. All measurements were performed upon custom screen-printed electrodes (SPE) from Flexmedical Solutions, incorporating a 5 mm carbon working electrode, carbon counter and a quasi-silver paste reference.

### ECL detection of L-GEM at varied pH

The ECL sensor was fabricated following our previously published procedure.<sup>13</sup> Briefly, the working electrode surface was modified by drop-casting a mixture of 0.5 mM [Ru(bpy)<sub>3</sub>]<sup>2+</sup> in a 0.2% w/v Nafion conductive film. After casting, gentle heating was applied to ensure rapid evaporation of any residual solvent and secure the complex to the electrode surface.

GEM loaded HNP were diluted in a 1:1 v/v ratio with either pH 7.4 or pH 12 0.1 M NaCl electrolyte to produce samples at the desired pH. For each measurement, 50 μL of the final solution was then used. All samples were stored at 2–8 °C when not in use. pH adjustments were made using 1 M NaOH or HCl as required.

### Subculture of human pancreatic cancer cells (BxPC-3)

BxPC-3 cells were grown in RPMI media supplemented with 10% foetal bovine serum and 1% penicillin streptomycin. Cells were grown in flasks incubated at 37 °C, 95% humidity and 5% CO<sub>2</sub>. Cells were grown until they reached 80% confluency, when they were subcultured into plates for the incubation with the L-GEM, HNPs and L-GEM bound onto the HNPs.

### Cellular internalisation with analytes

BxPC-3 cells were plated into 6-well plates at 5000 cells per well. Cells were incubated for 24 h before addition of HNP alone, L-GEM alone and L-GEM bound HNPs diluted in media, a control well of untreated cells was also used. Cells were further incubated for 24 h, before the media was removed and the cells were washed with phosphate buffered saline three times. The cells were then trypsinised (370 μL), once the cells were detached from the plate, they were diluted with 1 mL fresh media. This cellular suspension was transferred into Eppendorf tubes for the ECL analysis studies.

### ECL detection of L-GEM within BxPC-3CELLS

Cells inside Eppendorf tubes were either cooled to room temperature (20 °C) or incubated using an Eppendorf heating block to 44 °C and 66 °C before analysis. For ECL measurements, the cells were diluted in a 1:1 v/v ratio with the pH adjusted 0.1 M NaCl electrolyte (pH 7.4 or pH 12) to enable electrochemical detection. Following dilution, samples were maintained at their target temperature to ensure ECL analysis was conducted at the specified temperatures.

## Results and discussion

Initial electrochemical characterisation of the HNPs without drugs attached, revealed that no significant signal in the region of interest was observed (Fig. 2) and as such any anodic peaks present can be confidently attributed to the presence of the L-GEM. Under the same electrochemical conditions GEM produces an anodic peak within the region ~0.9 V *vs.* a pseudo-silver reference in the presence of pure AuNPs.<sup>15</sup> The AuNPs act as a catalyst, promoting GEM oxidation, which is typically weak at bare carbon surfaces and facilitating the production of an ECL signal.<sup>15,16</sup> This peak at ~0.9 V has previously been attributed to the electro-oxidation of the secondary amine present within GEM's structure. Oxidation of the secondary amine leads to the generation of the radical cation, the mechanism for GEM oxidation is shown in Scheme 1.<sup>15</sup> However, the direct detection of this oxidation peak at clinically relevant levels has been shown to be problematic and without the presence of AuNPs could not produce an ECL response due to the dimerization of the GEM radical as an alternative route to the ECL pathway (see Scheme 1).<sup>15,16</sup> Without the AuNP being in close proximity, no ECL was previously observed.

Here, it is observed that the HNP-GEM produces a similar oxidation peak within the same potential region of interest. As such, the Au shell of the HNPs also produce a similar catalytic enhancement towards GEM oxidation, resulting in the anodic peak observed at ~0.9 V *vs.* Ag (Fig. 2A). Given the enhancement effect provided by the catalytic properties of the HNPs, a similar enhancement toward ECL detection of L-GEM was envisioned. The ECL and CV behaviour of both HNP and L-GEM in the absence of [Ru(bpy)<sub>3</sub>]<sup>2+</sup> has been previously reported.<sup>16</sup>

With the ability to directly monitor unbound GEM previously demonstrated in the presence of the HNP,<sup>16</sup> it was necessary to ascertain whether the binding procedure would prevent L-GEM's ability to behave as a suitable co-reactant in this system. As previously determined,<sup>16</sup> to produce a recordable ECL signal the system must operate under alkaline conditions. Hence, as expected, no notable signal was recorded at a physiological pH of 7.4 (Fig. 2B). However, upon adjustment of the matrix pH a measurable signal, with a maximum ECL intensity emerges at a potential of ~1.1 V *vs.* Ag. This value aligns well with the previously obtained data,<sup>16</sup> with shift in potential arising due to the gold shell of the HNPs, similar to the phenomenon reported in the AuNP work.<sup>16</sup> L-GEM was observed to still behave as a co-reactant even when immobilized on the HNP surface *via* the Diels–Alder coupling (Fig. 2C), with an signal/background (S/B) ratio of ~5 recorded, this provides confidence in the ability to distinguish between when the L-GEM is fully bound to the HNP surface and when it has undergone the retro Diels–Alder reaction (after heat trigger) and been liberated, existing free in solution.

In order to serve as meaningful analytical tool in measuring drug release, ECL must be capable of monitoring drug release in biological systems such as *in vitro* in cells. This is something which currently is not achievable for these theranostic HNPs.



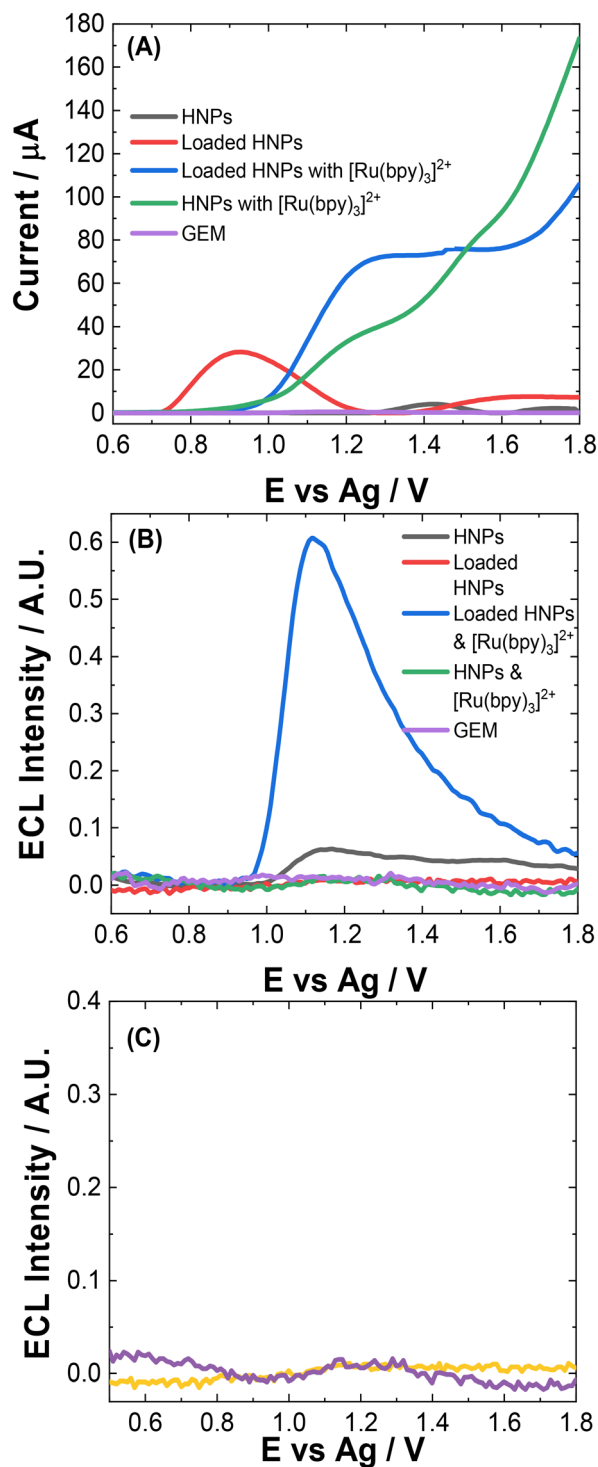


Fig. 2 ECL testing of HNP and drug loaded HNPs in solution. A) SW response obtained with non-loaded HNPs (black) and 26  $\mu\text{M}$  L-GEM loaded (red) HNPs, 26  $\mu\text{M}$  L-GEM (purple) upon bare carbon paste working electrode, 26  $\mu\text{M}$  GEM loaded (blue) HNPs upon a *via* 0.5 mM  $[\text{Ru}(\text{bpy})_3]^{2+}$  modified electrodes, non-loaded HNPs upon *via* blank 0.5 mM  $[\text{Ru}(\text{bpy})_3]^{2+}$  modified electrode (green) with a supporting electrolyte of 0.1 M NaCl, measurements were collected at a scan rate of 100  $\text{mV s}^{-1}$  across a potential range of  $0.6 \leq E \leq 1.6$  V vs. Ag. B) ECL signals obtained from (A) and (C) ECL from pH 7 non-loaded HNP (yellow) and 26  $\mu\text{M}$  L-GEM loaded (purple) HNPs in a supporting electrolyte of 0.1 M NaCl, measurements were collected at a scan rate of 100  $\text{mV s}^{-1}$  across a potential range of  $0.6 \leq E \leq 1.8$  V vs. Ag at a PMT bias of 0.6 V.



Scheme 1 Electrochemical pathway which the GMB radical can proceed down following electrocatalytic oxidation (a) and (b) at the AuNP surface, where (c) is the radical species, (d) is the dimerization product and (e) is the product of the ECL pathway alongside the required. Adapted from ref. 16.

Currently, the only indication drug release has occurred is based on drug efficacy increasing after induction of laser (and subsequent heating) in cells or *in vivo*, but the tools do not currently exist to confirm whether this release actually occurs inside cells in real-time, or whether another phenomenon is resulting in the therapeutic effect. Biological systems are intrinsically complex biological and therefore, it was important to test whether detection of the L-GEM was still possible in these matrices. Having demonstrated the ability to successfully monitor the immobilized L-GEM on the HNP under ideal electrochemical conditions, progression was made toward monitoring within human pancreatic cell lines (BxPC-3). Previous investigations have revealed the ability of ECL to monitor GEM within human pooled serum,<sup>15</sup> whilst alternative research has shown its compatibility with a variety of biological matrices including whole blood, urine, saliva and sweat.<sup>19–24</sup> Additionally, ECL has begun to emerge as a promising tool for cell analysis and as a microscopy technique and thus its translation toward drug release monitoring is inevitable.<sup>25,26</sup>

Preliminary assessment of the potential for drug release monitoring *via* temperature-controlled release with L-GEM loaded HNPs was performed. Analysis was undertaken either under natural cell pH (pH 7.4) or within the alkaline conditions (pH 12) necessary to facilitate the electrochemical detection of the L-GEM. Given the complexity of the genetic make-up of cells, it was necessary to establish the intrinsic signal attributed to the cellular make up prior to the addition of the L-GEM loaded HNP. This was carried out through analysis of control cells (with no treatment) which, as expected, produced an intrinsic signal (Fig. 3A and B). The intensity of this signal was observed to varying extents, both under natural cell conditions (Fig. 3A) and within pH modified (Fig. 3B) cell lines. However, the degree of this variation was not surprising, as it was influenced by the way in which the assessment was made given the drop-casting protocol currently employed, as well as the natural cell to cell variation.

Of note however was the consistent intensity difference between L-GEM containing cells (whether free or bound onto the HNP) compared with the control cell line under alkaline pH. Despite the high degree of natural cell variation, this negative difference in ECL intensity remained consistent





**Fig. 3** Investigation into *in vitro* monitoring of L-GEM release from HNP surface at elevated temperature *in vitro* in BxPC-3 cell lines. Results report the triplicate ECL average of  $n = 2$  cells analysed. Summary of maximum ECL intensities recorded from control cells with no drug treatment (green), 26  $\mu\text{M}$  L-GEM loaded cells (blue), unloaded HNPs (yellow) and 26  $\mu\text{M}$  L-GEM loaded HNPs in cells at A) pH 7.4 and B) pH 12 adjusted cells. Measurements were made upon the  $[\text{Ru}(\text{bpy})_3]^{2+}$  modified electrodes across at a scan rate of  $100 \text{ mV s}^{-1}$  across a potential range of  $0 \leq E \leq 1.8 \text{ V}$  vs. Ag at a PMT bias of 0.6 V.

(Fig. 3). As expected, given the electrochemical inactivity of L-GEM under physiological pH values, ECL interrogation of the spiked cell lines did not reveal any notable ability to monitor drug release across all temperature readings (Fig. 3A). However, when analysis was performed at pH 12, it revealed that variations in signal intensity could be monitored and used to draw the conclusion that upon the retro Diels Alder reaction at elevated temperatures, which theoretically initiates drug release, whereby a larger presence of L-GEM molecules were therefore liberated from the HNP surface, and free in solution, that this directly correlated to a higher ECL intensity (Fig. 3B). This is specifically observed at 44 °C, which is the temperature, at which the Diels–Alder construct was designed to undergo the retro reaction.<sup>1</sup> It was observed that, at higher temperatures (60 °C), the signal intensity dropped slightly, for BxPC-3 loaded with L-GEM alone (blue) and L-GEM bound HNPs (purple), which likely attributed to the thermal decomposition of L-GEM, which is noted to occur at similar temperatures under alkaline pH values in the literature.<sup>27</sup> Localised pH fluctuations will have an impact on the ECL intensity and this will require further research to ensure that the appropriate ECL luminophore is used and also that the impact of pH changes on its ECL performance is minimised over the expected pH ranges found with pancreatic cells and adjacent cells.

This exciting data confirms that ECL is a contender to offer a real time analytical detection of drug when released from nanoparticle surfaces or interiors. However, more work is required to translate this into quantitative data, as this report is based on qualitative analysis only. Previously work has shown that quantitative ECL analysis for GEM is possible using the process described here over the concentration range 6.25  $\mu\text{M}$  to 50  $\mu\text{M}$  GEM.<sup>16</sup> However, this proof of concept study offers a route to interrogate what happens to HNPs and their loaded drugs, GEM in this instance, upon delivery to the target cell.

Although the data presented are qualitative in nature, this is the first-time real-time detection of GEM released from the HNP has been detected. This is a major breakthrough in the nanomedicine world, where the ability to monitor drug release is highly reliant on diffusion assays through dialysis membranes and not real time measurements *in situ*. Whilst we have shown that qualitative measurement is now possible using this technique, the intent is to work towards quantitative measurement, which is the next step in this research journey. One major drawback in this study however, is the need to elevate the pH from 7.4 to pH 12 in order for drug detection to be possible. This, whilst not a substantive issue for *in vitro* analysis, unfortunately will rule out its use *in vivo*, where adjusting pH within a living system is not feasible and would mean that a modified ECL luminophore that reacts with L-GEM at physiological pH, such as some quantum dots<sup>28</sup> or an alternative metal, like osmium, iridium or rhenium could address this obstacle.<sup>29</sup> This short communication does highlight the potential of this approach for qualitative interrogation of the fate of drugs delivered *via* HNPs, and further work is underway to realise its potential in quantitative measurement.

This increase in ECL intensity with temperature variation allows for the hypothetical use of ECL toward drug release monitoring *in vivo*. Here we have determined that ECL can provide a suitable visualisation technique which could offer a viable solution for dose release monitoring toward precision medicine (and moving towards quantitative measurement). ECL over other spectroscopic techniques in the field offers the benefit of not only generating emission *in situ* but by negating the need for an external light source, it provides a visual monitoring strategy that could be monitoring using standard photography equipment. Fig. 4 demonstrates the visual emission observed within the cell lines, recorded *via* a standard mobile phone camera. As such, this provides an





**Fig. 4** Recording of ECL emission with A) 1 mM  $[\text{Ru}(\text{bpy})_3]^{2+}$  in solution and B) 0.5 mM  $[\text{Ru}(\text{bpy})_3]^{2+}$  film modified electrodes with 26  $\mu\text{M}$  L-GEM bound HNPs in BxPC-3 cell lines at pH 12. Recorded using an iPhone 12 Pro camera.

initial platform toward a lower cost monitoring strategy, which given this initial concept proof has the potential for huge benefit in dose monitoring strategies. The utility of alternative ECL luminophores for use within blood and other biological samples<sup>11,15,30</sup> also expands the potential applicability of this approach.

## Conclusions

These preliminary results provide a solid proof of concept for using ECL in the monitoring of thermally induced drug release. However, given the variation in signal intensity observed, particularly in regard to the intrinsic background signal of the cells, it is necessary for a much wider study to be performed to confidently establish the cell background level where a threshold intensity value could be established. What's more given the necessity to increase the pH value to alkaline values, this does limit this current system to *in vitro* application rather than *in vivo* analysis and as such, further work to modify the ECL luminophore to address this would also be necessary.

## Author contributions

CH and LD were responsible for the conceptualisation, investigation, supervision of the work as well as being responsible for the resources and writing, review and editing of the manuscript. KB and AO were responsible for the formal analysis and data curation as well as drafting the manuscript. All authors approved manuscript before submission.

## Conflicts of interest

There are no conflicts to declare.

## Data availability

All data underpinning this publication are openly available from the University of Strathclyde Knowledge Base at <https://doi.org/10.15129/b39a1879-2914-4999-8929-9ce358dbe9bb>.

## Acknowledgements

The authors would like to thank Tenovus Scotland (S20-05) for funding this work.

## References

- 1 Y. Liu, H. Xu, S. Bai, T. Chen, X. Ma, J. Lin, L. Sun, C. Gao, A. Wu and Q. Li, *Regener. Biomater.*, 2025, **12**, rbaf054.
- 2 K. Kokkinogoulis, A. Kollas, D. Simeonidis, P. Papakostas, K. Platoni, E. P. Efstathopoulos and M. Makropoulou, *Explor. Targeted Anti-Tumor Ther.*, 2025, **6**, 1002326.
- 3 A. Oluwasanmi, S. Lindsay, A. Curtis, Y. Perrie and C. Hoskins, *Int. J. Pharm.*, 2023, **644**, 123304.
- 4 A. Oluwasanmi, W. Al-Shakarchi, A. Manzur, M. H. Aldebasi, R. S. Elsin, M. K. Albusair, K. J. Haxton, A. D. M. Curtis and C. Hoskins, *J. Controlled Release*, 2017, **266**, 355–364.
- 5 M. Malekigorji, M. Alfahad, P. K. T. Lin, S. Jones, A. Curtis and C. Hoskins, *Nanoscale*, 2017, **9**(34), 12735–12745.
- 6 C. M. Barnett, M. Gueorguieva, M. R. Lees, D. J. McGarvey, R. J. Darton and C. Hoskins, *J. Nanopart. Res.*, 2012, **14**, 1170.
- 7 C. M. Barnett, M. Gueorguieva, M. R. Lees, D. J. McGarvey and C. Hoskins, *J. Nanopart. Res.*, 2013, **15**, 1706.
- 8 A. D. M. Curtis, M. Malekigorji, J. Holman, M. Skidmore and C. Hoskins, *J. Nanomed. Nanotechnol.*, 2015, **6**, 335.
- 9 A. Oluwasanmi, M. Malekigorji, S. Jones, A. Curtis and C. Hoskin, *RSC Adv.*, 2016, **6**, 95044–95054.
- 10 L. Dennany, R. J. Forster and J. F. Rusling, *J. Am. Chem. Soc.*, 2003, **125**(17), 5213–5218.
- 11 P. H. Shum and L. Dennany, *J. Electroanal. Chem.*, 2024, **973**, 118666.
- 12 K. Ino, T. Mockaitis, R. Shikuwa, K. Oba, K. Hiramoto, I. Morkvenaite-Vikonciene, H. Abe and H. Skiku, *Anal. Sci.*, 2025, **41**, 557–569.
- 13 G. Zou, X. Zhang, H. Li, C. Wang and B. Cai, *J. Mater. Chem. C*, 2025, **13**, 15796–15806.
- 14 Y. Yan, L. Ding, J. Ding, P. Zhou and B. Su, *ChemBioChem*, 2024, **25**(23), e202400389.
- 15 K. Brown and L. Dennany, *Sens. Actuators Rep.*, 2021, **3**, 100065.
- 16 K. Brown, A. Oluwasanmi, C. Hoskins and L. Dennany, *Bioelectrochemistry*, 2022, **146**, 108164.
- 17 M. M. Richter, *Chem. Rev.*, 2004, **104**, 3003–3036.
- 18 W. Miao, *Chem. Rev.*, 2008, **108**, 2506–2553.
- 19 A. J. Stewart, J. Hendry and L. Dennany, *Anal. Chem.*, 2015, **87**, 11847–11853.
- 20 A. J. Stewart, K. Brown and L. Dennany, *Anal. Chem.*, 2018, **90**, 12944–12950.
- 21 K. Brown, M. McMenemy, M. Palmer, M. J. Baker, D. W. Robinson, P. Allan and L. Dennany, *Anal. Chem.*, 2019, **91**, 12369–12376.
- 22 K. Brown, C. Jacquet, J. Biscay, P. Allan and L. Dennany, *Analyst*, 2020, **145**, 4295–4304.
- 23 E. Dokuzparmak, K. Brown and L. Dennany, *Analyst*, 2021, **146**, 3336–3345.
- 24 C. McLean, B. Tiller, R. Mansour, K. Brown, J. Windmill and L. Dennany, *J. Electroanal. Chem.*, 2022, **909**, 116149.
- 25 H. Ding, B. Su and D. Jiang, *ChemistryOpen*, 2022, **12**(5), e202200113.
- 26 A. Zanut, A. Fiorani, S. Rebecani, S. Kesarkar and G. Valenti, *Anal. Bioanal. Chem.*, 2019, **411**, 4375–4382.



- 27 R. Singh, A. K. Shakya, R. Naik and N. Shalan, *Int. J. Anal. Chem.*, 2015, **2015**, 862592.
- 28 S. M. O'Connor, L. Dennany and E. J. O'Reilly, *Bioelectrochemistry*, 2023, **149**, 108286.
- 29 K. Brown, C. Jacquet, J. Biscay, P. Allan and L. Dennany, *Anal. Chem.*, 2020, **92**(2), 2216–2223.
- 30 P. H. Shum and L. Dennany, *Analyst*, 2024, **149**, 2655–2663.

